THE JOURNAL OF PHYSICAL CHEMISTRY B

Article

pubs.acs.org/JPCB

Radiation Stability of Cations in Ionic Liquids. 1. Alkyl and Benzyl Derivatives of 5-Membered Ring Heterocycles

Ilya A. Shkrob,*[,†] Timothy W. Marin,[†,‡] Huimin Luo,[§] and Sheng Dai[∥]

[†]Chemical Sciences and Engineering Division, Argonne National Laboratory, 9700 South Cass Avenue, Argonne, Illinois 60439, United States

[‡]Chemistry Department, Benedictine University, 5700 College Road, Lisle, Illinois 60532, United States

[§]Energy and Transportation Science Division, Oak Ridge National Laboratory, Oak Ridge, Tennessee 37831, United States

[∥]Chemical Sciences Division, Oak Ridge National Laboratory, Oak Ridge, Tennessee 37831, United States

Supporting Information

ABSTRACT: In order to use hydrophobic room temperature ionic liquids (ILs) as diluents in nuclear separations for advanced fuel cycles, it is desirable to reduce the breakdown of the constituent ions caused by ionizing radiation. In this series, we survey radiation stability for different classes of organic cations used to formulate ILs. While radiolysis of 1-alkyl-3-methylimidazolium cations has been extensively studied, there have not been complementary studies of 1-benzyl derivatives of these cations nor organic cations that are derived from 5-membered ring heterocycles other than imidazole, such as 1,2,4-triazole and thiazole. In part 1, we establish the fragmentation pathways for such cations and quantify product yields for 2.5 MeV electron beam radiolysis of these aromatic cations. Radiolytic reduction of 1-benzyl cations derived from imidazole and 1,2,4-triazole is shown to cause the elimination of benzyl radicals from their electron adducts, whereas this elimination does not occur in the thiazole derivatives due to stabilization of the excess electron as a dimer radical cation. No such elimination occurs in the corresponding 1-alkyl derivatives, but there is significant C−N and C−C bond fragmentation in the aliphatic arms. As such bond dissociation reactions are irreversible, there is significant loss of 1-alkyl cations during the radiolysis. For 1-benzyl derivatives, this electronic excitation causes fragmentation of the C−N bonds in the benzyl arms with the release of the corresponding base and the benzyl carbocation that can subsequently attack this base or add to another cation. Such systems exhibit more predictable fragmentation patterns and yield well-defined products; some of the systems also exhibit increased radiation resistance. The C−N bond fragmentation in the reduced cations can be further suppressed through the use of appropriate electron scavengers, including acids and aromatic imide anions. The observed trends are rationalized using density functional theory calculations, and the implications of these results for the design of IL diluents are examined.

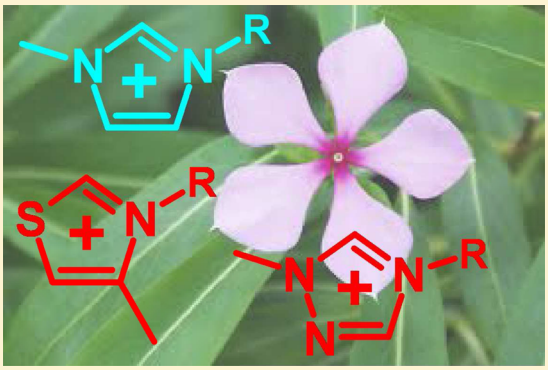

1. INTRODUCTION

Due to their outstanding properties, hydrophobic room-temperature ionic liquids (ILs)[1−4] hold promise to become next generation diluents in nuclear separations for advanced fuel cycles.[5−36] However, this application is conditional on minimizing the chemical damage to such diluents caused by ionizing radiation[37] that is generated by decaying radionuclides in the course of "wet" processing of spent nuclear fuel.[38−51]

At the inception of this technology in the early days of the Cold War, the pressing need to quickly develop practical solutions based on already-existing knowledge led to the entrenchment of methods that date well back into the previous century but continue to dominate present practice to this day. However, these methods are not sustainable if scaled up to meet the demands of the nuclear fuel cycle on the commercial scale, and new approaches are needed. At this juncture in the evolution of the nuclear cycle, a new class of infinitely pliable IL solvents is entering the stage and opportunities to reinvent the nuclear fuel cycle appear. This study offers a step in this direction. Which practically useful ILs are most radiation resistant? What factors control the stability of the constituent ions in such liquids? We will seek the answers to these questions with regard to organic cations,[52−56] thereby complementing our previous inquiry that focused on the radiation stability of anions.[52,53,57−59]

Previous mechanistic studies[52,56,60] and product analyses[39,40,42,59] indicate that the "weakest spot" of the ILs, in terms of their overall radiation stability, is *anion* (rather than cation) stability. Many of the anions that are used to constitute ILs readily fragment after electron detachment.[57] Such

Received: August 18, 2013
Revised: October 12, 2013
Published: October 22, 2013

Scheme 1. Structural Formulas for 1-R-3-Methylimidazolium ($RMeIm^+$), 1-R-3-Methyl-1,3,4-triazolium ($RMeT134^+$), 1-R-5-Methylthiazolium ($RMeTh^+$), Saccharinate (Sac^-), Bistriflimide (NTf_2^-), and Di(2-ethylhexyl)phosphate ($DEHP^-$)

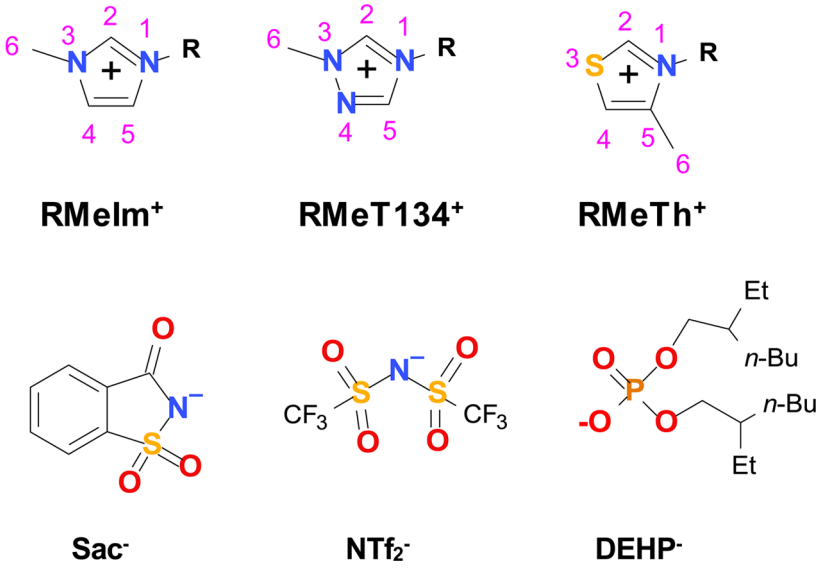

oxidative fragmentation can be reduced by judicious choice of anions.[58,59,61] In ref 58, we demonstrated that aromatic imide anions (like the saccharinate anion shown in Scheme 1) did not fragment after oxidation, reduction, and electronic excitation, so that, under practically relevant conditions (cumulative dose <0.5 MGy),[39] the loss of such anions was negligible. Certain polycyano anions, such as dicyanamide, 1,1,2,3,3-pentacyanopropenide, and 1,2,3,4,5-pentacyanocyclopentadienide, also exhibit exceptional radiation stability.[59] Our research continues, and more examples of stable anions can be identified. As the issue of anion stability has been partially addressed, we change our focus to the issue of cation stability. We stress that these two facets of radiation chemistry in ILs are intimately connected, as the radicals generated by anion decomposition react with the parent cations, and vice versa.

The typical organic cation (that can be represented as BR^+) consists of a positively charged base B (such as, for example, 1-methylimidazole) containing a heteroatom, such as P or N, and a side arm (R) that is attached to this heteroatom. The latter is typically an aliphatic chain. The longer the aliphatic arm, the more hydrophobic the IL. Since diluents used in nuclear processing must easily separate from aqueous raffinate and the constituent ions should not readily exchange with the inorganic ions present in the raffinate (e.g., refs 9, 12−14, 19, and 21), such IL diluents typically consist of a hydrophobic *cation* and a hydrophobic *anion* (such as bistriflimide, NTf_2^-, shown in Scheme 1). Radiation exposure causes electronic excitation and "ionization" of the ions: that is electron detachment from the anions (A^-) and electron attachment to the cations (C^+).

$$(A^-)^{**} \rightarrow A^{\bullet} + e^{-\bullet} \quad (1)$$

$$C^+ + e^{-\bullet} \rightarrow C^{\bullet} \quad (2)$$

In these energetic reactions, neutral $A^{\bullet}$ and $C^{\bullet}$ radicals are generated. Since the excitation energy per ionization event is large (>10 eV), the cation can also lose an electron ($e^{-\bullet}$), forming a short-lived radical dication $C^{2+\bullet}$ whose chemical stability is reduced due to strong Coulomb repulsion in the species.

$$(C^+)^{**} \rightarrow C^{2+\bullet} + e^{-\bullet} \quad (3)$$

Such radical dications typically decay by deprotonation from their long arms with the formation of a corresponding C-centered p-radical[52,56,60]

$$C^{2+\bullet}A^- \rightarrow C(-H)^{+\bullet} + H^{\delta+}A^{\delta-} \quad (4)$$

Such $C(-H)^{+\bullet}$ radicals recombine and disproportionate with other radicals, and the release of the proton increases the acidity of the IL diluent. While such reactions are detrimental, they do not necessarily disrupt the cation structure. The same generally relates to one-electron reduction of aromatic cations: the resulting $C^{\bullet}$ radicals, such as 2-imidazolyl from imidazolium derivatives (Scheme 2), are stable and become even more stable

Scheme 2. Main Types of Radicals Derived from 5-Atom Ring Cations

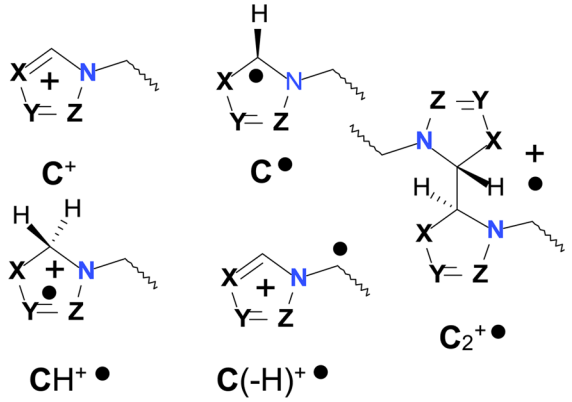

after protonation at carbon-2 (Scheme 2) that yields $CH^{+\bullet}$ radical cations, which can be viewed as products of hydrogen atom addition to the parent cations.

$$C^{\bullet} + H^{\delta+}A^{\delta-} \rightleftharpoons CH^{+\bullet} + A^- \quad (5)$$

These radicals can subsequently react with other reactive species, but there is no loss of functionality in the cation moiety.[60] Other pathways to stabilization of neutral radicals

dx.doi.org/10.1021/jp4082432 | J. Phys. Chem. B 2013, 117, 14372−14384

generated in reactions 1 and 2 involve their reactions with the like charged parent ions

$$\mathbf{A}^{\bullet} + \mathbf{A}^{-} \rightleftharpoons \mathbf{A}_2^{-\bullet} \quad (6)$$

$$\mathbf{C}^{\bullet} + \mathbf{C}^{+} \rightleftharpoons \mathbf{C}_2^{+\bullet} \quad (7)$$

The examples of reaction 6 are the formation of the $\sigma^2\sigma^{1*}$ N−N bound dimer radical anion for dicyanamide and C−C bound dimer radical anions of tricyanomethanide. Some examples of reaction 7 include the formation of $\sigma^2\sigma^{1*}$ C_2−C_2 bound dimer radical cations for 3-alkyl-1-methylimidazolium ($RMeIm^+$)[53,56] and π-sandwich dimer radical cations for 1-alkyl and 1-benzylpyridinium cations ($BzPy^+$, see part 2 of this study).[55]

Such reactions may or may not be detrimental, but they do not *fragment* these cations. In contrast, electronic excitation of cations can cause irreversible loss due to elimination of the aliphatic arm

$$\{BR^+\}^{**} \rightarrow BH^+ + R(-H) \quad (8)$$

This reaction yields a protonated base (BH^+) and a corresponding 1-olefin (see Scheme 1S in the Supporting Information).[56,60] A similar reaction can also involve unstable $\{BR^{\bullet}\}^*$ radical intermediates that are produced in energetic reaction 2:

$$\{BR^{\bullet}\}^* \rightarrow B + R^{\bullet} \quad (9)$$

Reaction 9 yields a free base that can be subsequently protonated by acid generated via deprotonation of the cations (see above)

$$B + H^{\delta+}\mathbf{A}^{\delta-} \rightleftharpoons BH^+\mathbf{A}^- \quad (10)$$

or catalyze deprotonation of other species, including the cations that have labile hydrogen (such as imidazolium cations, Scheme 1). Reactions 8 and 9 are irreversible. Since radiolysis is inevitable, the only way to reduce radiolytic damage without a sacrificial agent ("antirad") is to strive for reversibility of the reactions involved. For cations with aliphatic arms, little can be done to achieve such reversibility; however, in a more general case, alternative reaction

$$\{BR^+\}^{**} \rightarrow B + R^+ \quad (11)$$

can be preferred to reaction 8. Reaction 11 could, in fact, be the intermediate stage of reaction 8 for cations with aliphatic arms (Scheme 1S, Supporting Information): the carbocations of normal alkanes are unstable to deprotonation, so the leaving group loses a proton to the base released in reaction 11. When the stability of this carbocation increases, this deprotonation may not occur. Unlike reaction 8, reaction 11 is reversible; this reaction is the very quaternization through which these organic cations are synthesized:

$$B + R^+ \rightarrow BR^+ \quad (12)$$

Unless the geminate partners generated in reaction 11 escape each other or react with other species (in particular, base B can become protonated via reaction 10 and carbocation R^+ can attach to aromatic rings of the parent ions, section 4.2), this pair recombines and regenerates the parent cation.

This examination suggests that a possible approach to improving cation stability is by replacing the *n*-alkyl arms with arms that yield more stable carbocations, such as benzyl (Bz) arms. The problem with this approach is that any such stabilization inadvertently stabilizes radical $R^{\bullet}$ that is released in reaction 9, so while reaction 8 is suppressed and reaction 9 becomes (potentially) reversible, there is increased fragmentation of the cation via reaction 9, which offsets these advantages. Indeed, the reduction of the R_3NBz^+ cation by a hydrated electron in aqueous solutions yields benzyl radicals:[62−64] the intermediate $R_3NBz^{\bullet}$ radical dissociates to R_3N and $Bz^{\bullet}$. It appears that such contradictory requirements derail this strategy.

However, such a situation is not inevitable. First, stabilization of the electron adducts generated in reaction 2 via reaction 7 can considerably change the energetics. In part 2 of this series,[55] we demonstrate that this is indeed the case for 1-benzylpyridinium that avoids reaction 9 due to the occurrence of rapid dimerization. Another possible strategy is avoidance of reaction 2 itself provided that the electrons released in reactions 1 and 3 are scavenged by *anions* rather than *cations*:

$$\mathbf{A}^- + e^{-\bullet} \rightarrow \mathbf{A}^{2-\bullet} \quad (13)$$

In ref 58, we demonstrated that aromatic imides competitively scavenge electrons with 1-alkyl-3-methylimidazolium cations, and the resulting radical dianions (being strong bases) protonate radical anions (that can be formally considered as H atom adducts of the parent anions), e.g.,

$$\mathbf{A}^{2-\bullet} + H^{\delta+}\mathbf{A}^{\delta-} \rightarrow \mathbf{A}H^{-\bullet} + \mathbf{A}^- \quad (14)$$

Similar reactions were observed for polynitrile anions.[59] Third, only a few types of aromatic cations have been studied with regard to their radiation stability, so it is not known how general these conclusions are.

To address these concerns, we studied radiolysis of two less common aromatic cations that are based on 1,2,4-triazole and thiazole (see Scheme 1) and compared them to the more common imidazole based cations. For uniformity, the atom numbering convention shown in Scheme 1 is used in the following, breaking with the conventional way of numbering atoms in these heterocycles. The numbering of atoms in the 1-benzyl derivatives follows Figure 1. Both 1-alkyl and 1-benzyl derivatives of the corresponding cations were synthesized, and their radiation chemistry was studied using electron paramagnetic spectroscopy (EPR) and by product analysis. Our study indicates that, even among the cations that are based on 5-membered ring heterocycles, significant differences in the behavior are observed. In part 2,[55] we demonstrate that pyridinium cations are still more different in their behavior from these species. Still, more difference can be expected from other heterocyclic compounds. Our goal is less to chart this rich chemistry than to formulate the design principles that can underlie further optimization. The vast majority of IL studies involved only a few classes of organic ions, while there is no guarantee that the optimum that we seek is circumscribed by these classes.

To save space, many of the supporting tables, figures, details of synthetic and analytical protocols, and a list of abbreviations have been placed in the Supporting Information. When referenced in the text, these materials have the designator "S", as in Figure 1S (Supporting Information).

2. EXPERIMENTAL AND COMPUTATIONAL METHODS

All reagents were obtained from Aldrich and used as supplied without further purification. The details of synthetic procedures (section 1S, Supporting Information), melting points for crystalline hexafluorophosphates (Table 1S, Supporting Information), nuclear magnetic resonance (NMR) spectra (Table 2S, Scheme 2S, and Figures 1S and 2S, Supporting

dx.doi.org/10.1021/jp4082432 | J. Phys. Chem. B 2013, 117, 14372−14384

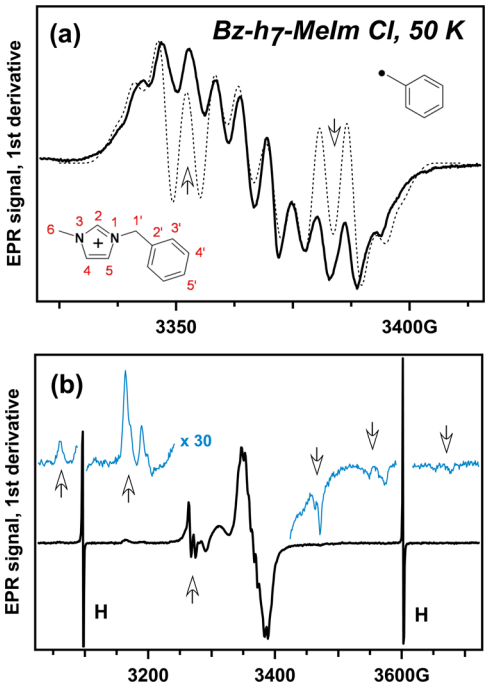

Figure 1. First-derivative EPR spectrum of irradiated frozen BzMeIm Cl observed at 50 K (0.02 mW, 2.5 MeV electron beam radiolysis at 77 K). In panel a, the bold line designates the experimental spectrum and the dashed line is the simulated spectrum of the benzyl radical. The arrows indicate centroids of the doublet of lines from the $-H_{1'}$ radical that are obscured by the benzyl radical. In panel b, a wide sweep EPR spectrum obtained at 2 mW is shown. In addition to the features shown in panel a, there are six groups of lines from the $^{35,37}Cl_2^{-\bullet}$ center (indicated by arrows) and a doublet of lines from trapped hydrogen atoms.

Information), and mass peaks for ionic compounds (Table 3S, Supporting Information) are given in the Supporting Information. 1-Alkyl and 1-benzyl thiazolium and triazolium based cations were synthesized following the methods given by Dai and co-workers.[65,66] For 1-benzyl-3-methylimidazolium based ILs, selectively isotopomers containing deuterated benzyl moieties (Bz-d_7–MeIm$^+$) were also synthesized. Crystalline hexafluorophosphate of these RMeU$^+$ compounds (where U is the heterocycle base) were selected, as in radiolysis of such salts there is relatively little derivatization of the cations by fragments of dissociated anions, whereas for many other ionic compounds such reactions are prevalent (see part 2).[55] For this reason, these RMeU PF_6 compounds are particularly suitable to study *cation* stability, despite these compounds being crystalline rather than liquid at room temperature. This distinction becomes unimportant for low-temperature EPR studies, as all of these compounds are solids at 77 K.

For product analysis, the samples were evacuated and sealed in water-cooled borosilicate NMR tubes (O.D. 5 mm) and irradiated by 2.5 MeV electrons to a total dose of 2.5–4.5 MGy using a dose rate of 6.8 kGy/s (1 Gy = 1 J/kg of the absorbed energy). The irradiation dose was estimated using the Fricke dosimeter, and the stopping power of the fast electrons was corrected by the electron density of the IL. The electron beam traveled through 1 cm of water before hitting this sample tube and was sufficiently dispersed to irradiate the vertical column of 2.5 cm. These samples were irradiated at room temperature, as this is the most practically important regime, whereas spectroscopic observations were carried out in frozen samples, to prevent thermal decay of radiolytically generated radicals in the matrix.

^1H, ^{13}C, ^{19}F, and ^{31}P NMR spectra were obtained in dimethylsulfoxide-d_6 (DMSO-d_6), using an Avance DMX 500 MHz spectrometer (Bruker); for ^1H and ^{13}C, the chemical shifts are given vs tetramethylsilane (TMS). ^1H–^1H COSY two-dimensional NMR spectroscopies were used to establish connectivity. For ^{19}F and ^{31}P NMR, the chemical shifts are given relative to $CFCl_3$ and H_3PO_3 standards, respectively.

Tandem electrospray ionization mass spectra (ESI MS_n) were obtained using a Thermo Scientific LCQ Fleet ion trap mass spectrometer operating either in positive or negative modes ($MS_n^{\pm}$). MS_1 corresponds to the first quadrupole and MS_2 corresponds to collision induced dissociation (of mass selected ions) modes of operation. Liquid samples were injected directly into dilute acetonitrile solutions. $(\mathbf{CA})_n\mathbf{C}^+$ and $(\mathbf{CA})_n\mathbf{A}^-$ cluster ion series (n = 0–8) were detected, and in some cases involved product ions. In section 4.2.1, only n = 0 ions of each series are reported.

For ESI MS analysis, radiolyzed samples were dissolved in a minimal amount of DMSO-d_6 and further diluted by acetonitrile to obtain 2 wt % solutions. Liquid chromatography was used to separate and identify isobaric products. To this end, a 2 μL aliquot was analyzed using high-performance liquid chromatography (ThermoScientific Accela suit) with ESI MS_1^+ detection. A weak cation exchange phase with carboxylate surface groups was used (Thermo Scientific WCX-1 phase; 120 Å pore, size 3 μm; 3 mm bore, 15 cm length) for isothermal elution at 0.2 mL/min; acetonitrile containing 0.1 wt % formic acid was used as an eluent.

For matrix isolation EPR spectroscopy, the samples were frozen by rapid immersion in liquid nitrogen and irradiated to 3 kGy at 77 K. The radicals were observed using a 9.44 GHz Bruker ESP300E spectrometer, with the sample placed in a flow helium cryostat (Oxford Instruments CF935). The magnetic field and the hyperfine coupling constants (hfcc's) are given in units of Gauss (1 G = 10^{-4} T). If not stated otherwise, the first-derivative EPR spectra were obtained at 50 K using 2 G modulation at 100 kHz. The microwave power is indicated in the figures. The radiation-induced EPR signal from the E_γ' center in the Suprasil sample tubes (that frequently overlapped with the resonance lines of organic radicals) is shadowed white in the EPR spectra.

The calculations of the hfcc's and radical structures were carried out using a density functional theory (DFT) method with the B3LYP functional[67,68] and 6-31+G(d,p) basis set from Gaussian 03.[69] In the following, a_{iso} denotes the isotropic hfcc corresponding to the hfc tensor and **B** denotes the anisotropic part. Powder EPR spectra were simulated using first-order perturbation theory. For convenience, the principal values of the **g**-tensor are reported as $\delta\mathbf{g}_{\nu\nu} = (\mathbf{g}_{\nu\nu} - 2\cdot\mathbf{1}) \times 10^4$, where ν = x, y, z are the principal axes (the molecular frame).

3. PRELIMINARY CONSIDERATIONS

In section 1, we gave a general introduction to radiation induced reactions of aromatic cations, and in section 4, we demonstrate that this general scheme (that was originally suggested for 1-alkyl-3-methylimidazolium cations)[53,54,56] relates to other RMeU$^+$ cations. To facilitate spectral identification, DFT was used to compute energetics (Table 4S, Supporting Information), optimize geometries (Table 5S and Figures 3S–6S, Supporting Information), and compute magnetic properties (Tables 5S–7S, Supporting Information)

dx.doi.org/10.1021/jp4082432 | J. Phys. Chem. B 2013, 117, 14372–14384

Table 1. Gas-Phase Energetics for Selected Methyl and Ethyl Substituted Cations (RMeU$^+$) and Their Derivatives (Optimized Geometry, B3LYP/6-31+G(d,p) Calculation)

U	R	IP[a] (eV)	D(C−H)[b] (eV)	PA[c] (eV)	ϕ[d] (deg)	a_{iso}[e] (G)	D(C−C)[f] (eV)	r(C−C)[g] (Å)	D(C−H)[h] (eV)
Im	Me	3.94	1.76	11.43	46.9	24.9	0.42	1.704	4.91
	Et	4.29	2.05	11.37	46.2	24.8	0.83	1.714	3.93
T134	Me	4.45	1.57	10.72	48.9	26.6	0.54	2.769	4.55[i]
	Et	4.29	1.61	10.92	48.5	36.6	0.60	2.741	4.38
Th	Me	4.79	2.15	10.97	41.5	7.6	0.85	1.638	4.27[j]
	Et	4.72	2.16	11.04	42.0	9.5	0.88	1.640	4.25

[a]Adiabatic ionization potential for $\mathbf{C}^\bullet$. [b]C_2−H bond dissociation energy in $\mathbf{CH}^{+\bullet}$. [c]Proton affinity of $C^\bullet$. [d]Trigonality at carbon-2 in $\mathbf{C}^\bullet$ (that is, the deviation of H_2−C_2−N_1−X_3 dihedral angle from 180°). [e]Isotropic hfcc in $^1H_2$ of $\mathbf{C}^\bullet$. [f]C_2−C_2 bond dissociation energy in $\mathbf{C}_2^{+\bullet}$ (C_2 symmetry). [g]C_2−C_2 bond distance in $\mathbf{C}_2^{+\bullet}$. [h]Bond dissociation energy for N(1)CH_α atom abstraction from $\mathbf{C}^+$. [i]N(3)Me abstraction. [j]C(5)Me abstraction.

of the gas-phase radicals. To simplify computations, methyl and ethyl substituted radicals were examined. The structures of these radicals are shown in Figures 3S−6S (Supporting Information), and their simulated EPR spectra are shown in Figures 7S−10S (Supporting Information).

As seen from Table 1, the electron affinities of gas-phase RMeIm$^+$ and RMeT134$^+$ cations (that is, ionization potentials of the corresponding radicals) are comparable, while the RMeTh$^+$ cations are *stronger* electron acceptors. The resulting $\mathbf{C}^\bullet$ σ-radicals have trigonal carbon-2 atoms. The trigonal distortion increases from EtMeTh$^\bullet$ to EtMeIm$^\bullet$ to EtMeT134$^\bullet$, and the isotropic hfcc in $^1H_2$ proton increases from 9.5 to 25 to 36.6 G, respectively (structure i in Figures 4S and 6S, Supporting Information). This increase has a strong effect on the appearance of the simulated EPR spectra for these $\mathbf{C}^\bullet$ radicals, as shown in Figure 7S (Supporting Information).

The DFT calculations also suggest that reaction 7 is always exergonic in the gas phase. The lowest energy $\mathbf{C}_2^{+\bullet}$ radicals have C_2 symmetry and a $\sigma^2\sigma^{*1}$ (three-electron) bond between two carbon-2 atoms. The $(\mathrm{EtMeTh})_2^{+\bullet}$ cation has the shortest C_2−C_2 bond (1.64 Å) and the greatest binding energy (0.88 eV; Figure 6S, Supporting Information, structure ii) that is followed by $(\mathrm{EtMeIm})_2^{+\bullet}$ (1.71 Å and 0.83 eV, respectively). Due to the strong trigonal distortion in the monomer radical, for $(\mathrm{EtMeT134})_2^{+\bullet}$, the binding energy is only 0.6 eV and the C_2−C_2 distance is 2.77 Å, so the binding motif is equally resembling that of a π-sandwich (structure ii in Figure 4S, Supporting Information). As there is equal sharing of the unpaired electron density between the two units, the resulting EPR spectra are poorly resolved singlets (Figure 7S, Supporting Information). For the EtMeTh$^\bullet$ and $(\mathrm{EtMeTh})_2^{+\bullet}$ species, the EPR spectra for the $\mathbf{C}^\bullet$ and $\mathbf{C}_2^{+\bullet}$ radicals look very similar (due to small trigonal distortion in the σ-radical). In general, one can expect that lower temperature favors $\sigma\sigma^*$ bond formation, whereas thermal motion at room temperature weakens this binding; i.e., matrix isolation EPR is a particularly suitable method to probe for the occurrence of the dimerization.

The DFT calculations presented in Table 4S (Supporting Information) indicate that the lowest energy H atom adduct is always at carbon-2 (structure iii in Figures 3S, Supporting Information) and the corresponding EPR spectra are triplets from the two magnetically equivalent $^1H_2$ protons (Tables 5S and 6S and Figures 3S−6S, Supporting Information). The weakest C−H bond in the EtMeU$^+$ cations is always at the C_α carbon in the long arm, although for EtMeTh$^+$ the abstraction of hydrogen from methyl-4 is comparable energetically (Table 4S, Supporting Information). The corresponding EPR spectra are simulated in Figures 8S and 9S (Supporting Information).

The atom numbering convention for benzyl derivatives is shown in Figure 1a. All electron adducts of the BzMeU$^+$ cations dissociate in the gas phase (reaction 9). The estimated hfcc's for benzyl radicals agreed well with the experimental estimates in the literature (Figure 1a). DFT calculations (Table 7S, Supporting Information) suggest that H atom addition to C_2 carbon in the imidazole ring is more exergonic than H atom addition to $C_{3'}$ and $C_{5'}$ atoms in the phenyl ring. Abstraction of a $H_{1'}$ atom from the methylene group in the benzyl arm yields a $\mathbf{C}(-\mathrm{H})^\bullet$ radical with a single large hfcc in the remaining proton (Table 7S, Supporting Information), and the corresponding EPR spectrum is a doublet that "collapses" to a singlet line for the corresponding Bz-d_7−MeIm$^+$ isotopomer, as shown in Figure 10S (Supporting Information). (The deuteron is a spin-1 nucleus with a hfcc that is only 15.3% of the corresponding proton hfcc. Consequently, the EPR line "collapses" upon H/D substitution.) The H adducts and H loss radicals assume a "propeller" geometry in which the phenyl ring in the benzyl arm is perpendicular to the plane of a heterocycle ring.

4. RESULTS AND DISCUSSION

4.1. EPR Spectroscopy of Frozen Samples. *4.1.1. 1-Benzyl-3-methylimidazolium Compounds.* We begin our examination with EPR studies of 1-benzyl-3-methylimidazolium (BzMeIm$^+$) compounds; the 1-alkyl-3-methylimidazolium compounds have been examined in our previous studies.[52,53,56]

Figure 1 exhibits EPR spectra of irradiated frozen BzMeIm Cl. There are three groups of resonance lines: (i) the doublet of trapped H atoms (Figure 1b), (ii) a double sextet of lines from $Cl_2^{-\bullet}$ (present as a 3:1 mixture of ^{35}Cl and ^{37}Cl isotopes, both of which have spin-3/2 and slightly different nuclear magnetic moments, Figure 1b), and (iii) a well-resolved EPR spectrum of the benzyl radical (simulated in Figure 1a).

Comparison of simulated (dashed line) and observed spectra (solid line) from the benzyl radical in Figure 1a hints at the presence of a hidden doublet (indicated with arrows in Figure 1a) that we attribute to a −H(1′) loss radical (section 3 and Figure 10S, Supporting Information). In irradiated RMeIm Cl (R = ethyl, butyl), the $Cl_2^{-\bullet}$ radical was not observed,[57] as the chlorine atom generated in reaction 1 abstracts H from the aliphatic arm, yielding $\mathbf{C}(-\mathrm{H})^{+\bullet}$ radicals.[70] This reaction occurs more rapidly than binding of this chlorine atom to a chloride anion, yielding $Cl_2^{-\bullet}$. This is, apparently, not the case in BzMeIm Cl (and, as shown in part 2,[55] also in 1-benzylpyridinium chloride), although the energy of the $C_{1'}$−H bond in BzMeIm$^+$ is not substantially different from the energy of the C_α−H bond in RMeIm$^+$ cations.

The formation of the benzyl radical was also observed in other irradiated BzMeIm$^+$ compounds. Figure 2 shows EPR

dx.doi.org/10.1021/jp4082432 | J. Phys. Chem. B 2013, 117, 14372−14384

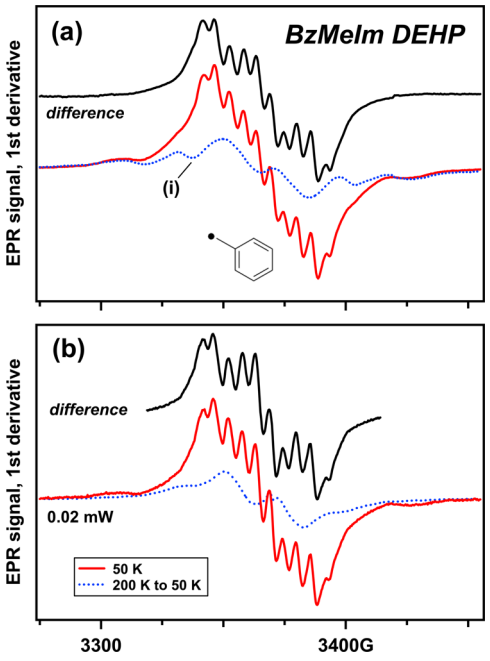

Figure 2. The solid red line in both of the panels indicates the first-derivative EPR spectra of irradiated frozen BzMeIm DEHP (Scheme 1) obtained at 50 K and 0.02 mW. Panel a: The dashed line is the scaled EPR spectrum of irradiated HDEHP, and the black trace is the difference of these two spectra. Panel b: The dashed blue line is the EPR spectrum of the sample warmed to 200 K and then cooled back to 50 K. Subtracting the spectra before and after this 200 K warming produces the trace shown at the top. The two difference traces are mainly from the benzyl radical.

spectra obtained in radiolysis of BzMeIm DEHP (Scheme 1). The pattern of the $Bz^{\bullet}$ radical is observed, with the H loss radical of $DEHP^{-}$ contributing to the background (Figure 2a). The latter radical has an EPR spectrum similar to the one observed in other DEHP compounds,[61] and it can be removed from the EPR spectrum by subtraction, as it persists at 200 K while the benzyl radical decays (Figure 2b). The benzyl radical was also observed in irradiated BzMeIm NTf_2 (Figures 11S and 12S(a), Supporting Information) and BzMeIm PF_6 (not shown), persisting until these samples were warmed to 175 K. The resonance lines of the benzyl radical overlap with the resonance lines of anion-derived radicals, such as $^{\bullet}CF_3$ and $^{\bullet}CF_2SO_2NTf$ in Figure 11S(b) (Supporting Information).

The characteristic pattern of this benzyl-h_7 radical was not observed for the corresponding Bz-d_7–MeIm isotopomer (dashed trace in Figure 12S(a), Supporting Information). This narrowing reveals interfering EPR lines from radicals that are derived from the 1-methylimidazolium moiety whose EPR spectra are not affected by deuteration in the benzyl group. The nature of these radicals can be discerned by warming the sample (Figures 12S, Supporting Information). When Bz-d_7–MeIm NTf_2 is warmed to 200 K, the EPR spectrum exhibits two groups of lines whose centroids are separated by 60 G, which we attribute to the D atom carbon-2 adduct shown in the inset (Figure 12S(b), Supporting Information). In none of these systems did we observe the $\mathbf{C}^{\bullet}$ radical, suggesting that reaction 9 readily occurs even at low temperature.

Can this fragmentation be avoided? The following results indicate that the fragmentation does not occur when an efficient electron acceptor is present in the IL. Only the H atom adduct of $MeHIm^{+}$ was observed in irradiated MeHIm BF_4:H_3O^{+}, which contained a protic impurity; a similar adduct and greatly decreased yield of the benzyl radical was observed in irradiated BzMeIm BF_4:H_3O^{+} (Figure 13S, Supporting Information). In this H_3O^{+}-doped compound, electrons are preferentially scavenged by hydronium ions (in preference to aromatic cations)[61] and the released H atoms promptly attach to the imidazolium ring, forming carbon-2 adducts.

Reactions 2 and 9 can also be suppressed by a judicious choice of the anion (section 1). Figure 3 exhibits EPR spectra

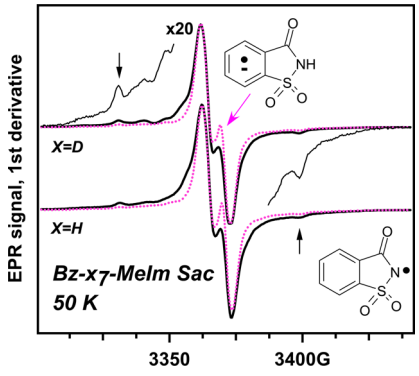

Figure 3. First-derivative EPR spectra of Bz-x_7–MeIm Sac (x = H and D) obtained at 2 mW (solid lines) and 0.02 mW (dashed lines) at 50 K. The central "split" doublet is from the $\mathbf{AH}^{-\bullet}$ radical, and the resonance lines indicated by the arrows are the outer lines of the imidyl radical ($\mathbf{A}^{\bullet}$). The structures of these species are shown in the insets in the plot.

obtained in irradiated BzMeIm Sac (Scheme 1). As shown in our previous study,[58] saccharinate readily accepts the electron (reactions 13 and 14) and the hole (reaction 1). The resulting $\mathbf{A}^{\bullet}$ and $\mathbf{AH}^{+\bullet}$ species (whose spectral signatures are known from previous studies)[58] are observed in the EPR spectra, whereas the benzyl radicals are not observed (Figure 3). Thus, in BzMeIm Sac, the saccharinate anion scavenges both electrons and holes, and reductive fragmentation of the $BzMeIm^{+}$ cation is prevented. While the occurrence of reaction 9 is an obstacle, it is not an insurmountable one.

4.1.2. Triazolium and Thiazolium Based Cations. Figure 4 exhibits EPR spectra from irradiated hexafluorophosphate salts of the 1-alkyl substituted cations shown in Scheme 1.

For BuMeIm PF_6, the doublet from the $\mathbf{C}^{\bullet}$ radical yields the largest contribution to this EPR spectrum, with a weaker contribution from the $\mathbf{C}(-H)^{+\bullet}$ radical observed in the spectral wings. The latter contribution is considerably greater for $RMeT134^{+}$ compounds. When the irradiated EtMeT134 PF_6 is gradually warmed to 175 K (Figure 14S, Supporting Information), there is radical decay, and the residual species has an EPR spectrum corresponding to the $\mathbf{C}(-H)^{+\bullet}$ radical at C_{α} in the ethyl arm (Figure 8S(b), Supporting Information); the same progression is also observed for BuMeT134 PF_6, which also yields a $\mathbf{C}(-H)^{+\bullet}$ radical (Figure 15S, Supporting Information). When the EPR spectrum of these $\mathbf{C}(-H)^{+\bullet}$ radicals (in the samples that are warmed to 175 K and then cooled to 50 K) is subtracted from the EPR spectra observed at 50 K (before warming), the difference EPR spectrum strongly (see Figure 5) resembles simulated EPR spectra for the corresponding $\mathbf{C}^{\bullet}$ radical, with its large hfcc coupling in the H_2 proton due to strong trigonal distortion in carbon-2 of the triazolium ring (section 3 and Figure 7S, Supporting

dx.doi.org/10.1021/jp4082432 | J. Phys. Chem. B 2013, 117, 14372–14384

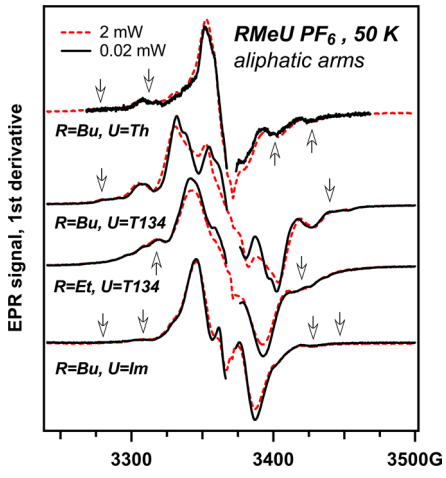

Figure 4. First-derivative EPR spectra observed in irradiated RMeU PF_6 compounds obtained at 50 K, using a microwave power of 0.02 mW (solid line) and 2 mW (dashed line). The aliphatic arm (R) and the heterocycle base (U) are indicated in the plot. The open arrows indicate the selected resonance lines of the $C(-H)^{+\bullet}$ radicals.

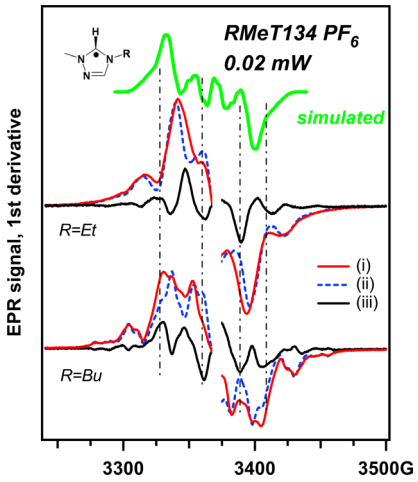

Figure 5. First-derivative EPR spectra observed in irradiated EtMeT134 PF_6 and BuMeT134 PF_6 obtained at 50 K using a microwave power of 0.02 mW, (i) before and (ii) after cycling the sample temperature to 175 K. Traces iii are the difference traces. A simulated spectrum of the electron adduct of EtMeT134 is shown at the top. The dash-dot vertical lines are guides for the eye.

Information). We conclude that the radiation chemistry of $RMeIm^+$ and $RMeT134^+$ is similar.

In irradiated BuMeTh PF_6, the lines of the corresponding H loss radical are observed, but there is also a narrow, unresolved singlet that can be attributed either to $\mathbf{C}^\bullet$ or $\mathbf{C}_2^{+\bullet}$ radicals (section 3 and Figure 7S, Supporting Information). Since these two radical species have similar patterns, EPR spectroscopy does not indicate which radical is formed. Warming of the sample to 200 K yields the progression shown in Figure 16S (Supporting Information). As the temperature increases, the intensity of the narrow singlet decreases, suggesting radical decay. The species observed above 150 K exhibits the characteristic pattern of $C(-H)^{+\bullet}$ radicals (Figure 8S(b), Supporting Information). There is no indication for the formation of the H adducts. For $RMeIm^+$ compounds, both $\mathbf{C}^\bullet$ and $\mathbf{C}_2^{+\bullet}$ radicals can be observed in different systems, depending on the counteranion, as the equilibrium reaction 7 can be shifted either way, depending on the strength of the solvation of the parent cation and the dimer radical cation.[53] In these previously studied systems, only $\mathbf{C}^\bullet$ radicals transformed to $\mathbf{CH}^{+\bullet}$ adducts (reaction 5), whereas the H adduct has not been observed in systems yielding $\mathbf{C}_2^{+\bullet}$ radical cations. Provided that this empirical rule also applies to $RMeTh^+$ cations, our observations indirectly suggest that the electron is trapped as a dimer radical cation.

In Figure 6, we compare EPR spectra observed in irradiated BzMeTh PF_6 and BzMeT134 PF_6. The predominant feature in both of these traces is an unresolved singlet. When the BzMeT134 PF_6 sample is warmed to 200 K, the rotation of radicals in the solid matrix becomes less arrested (Figure 17S, Supporting Information), and the fully resolved EPR spectrum of the benzyl radical is observed, with weaker signals from the $\mathbf{CH}^{+\bullet}$ radicals in the wings. Cooling of the sample back to 50 K once again yields the unresolved singlet; i.e., these spectral transformations are reversible (Figure 17S, Supporting Information). These observations indicate that $BzMeT134^+$ (like $BzMeIm^+$ in section 4.1.1) undergoes dissociative electron attachment, reaction 9.

In contrast, no resonance lines from the benzyl radical were observed when the irradiated BzMeTh PF_6 was subjected to the thermal annealing (Figure 18S, Supporting Information). Our DFT calculations suggest that in the gas phase the $BzMeU^\bullet$ radicals undergo reaction 9 (section 3), whereas this dissociation is not experimentally observed. In part 2,[55] we demonstrate that the $BzPy^+$ cation also exhibits this anomalous behavior and argue that the elimination of the benzyl radical is inhibited through the formation of a π-sandwich dimer radical cation in which the excess electron is trapped by two pyridinium moieties. Apparently, the electron center needs to be stabilized through charge delocalization to avoid reaction 9. Given that the C_2-C_2 bond in the $(RMeU)_2^{+\bullet}$ radical cations is the strongest for thiazolium derivatives (since 5-methyl substitution presents less steric hindrance than 3-methyl substitution), thiazolium compounds are more likely to yield the $\mathbf{C}_2^{+\bullet}$ radical cations than other $BzMeU^+$ cations.

We suggest that dimerization increases the stability toward $Bz^\bullet$ elimination both for reduced $BzPy^+$ and $BzMeTh^+$. Another interesting feature of these EPR spectra is the absence of the doublet from the $C(-H)^{+\bullet}$ radicals (the resonance lines indicated by the arrows in Figures 6 and 18S (Supporting Information) originate from the outer resonance lines in the $\mathbf{CH}^{+\bullet}$ radicals, Figure 10S, Supporting Information). Using EPR spectroscopy of isotope-substituted $BzPy^+$, in part 2,[55] we demonstrate that $BzPy^+$ cations trap positive charge as $(BzPy)_2^{3+\bullet}$ radicals in which the excess positive charge is shared between two phenyl rings in a π-sandwich dimer. This species was also recognized through its characteristic charge-resonance band in pulse radiolysis–transient absorption experiments.[55] The resulting radical is resistant to deprotonation reaction 4, which accounts for the suppressed $C(-H)^\bullet$ radical formation. It seems likely that the same mechanism is responsible for the suppression of the $C(-H)^\bullet$ radical formation for $BzMeTh^+$.

Summarizing these EPR observations, it appears that triazolium and imidazolium based cations have similar radiation chemistry, whereas thiazolium derivatives have somewhat different chemistry that can be traced to the lower trigonal distortion in the corresponding electron adduct that facilitates C_2-C_2 bond formation with the parent cation, reaction 7. The formation of $(BzMeTh)_2^{+\bullet}$ stabilizes the reduced species and

dx.doi.org/10.1021/jp4082432 | J. Phys. Chem. B 2013, 117, 14372–14384

prevents elimination of the benzyl radical; the monomer radicals would promptly eliminate the benzyl radical, like other such $\mathbf{C}^{\bullet}$ radicals.

4.2. Product Analyses. *4.2.1. Electrospray Ionization Mass Spectrometry.* Mass spectrometry of irradiated RMeU PF_6 compounds provides further insights into their radiation chemistry. Typical mass spectra are shown in Figure 7 where

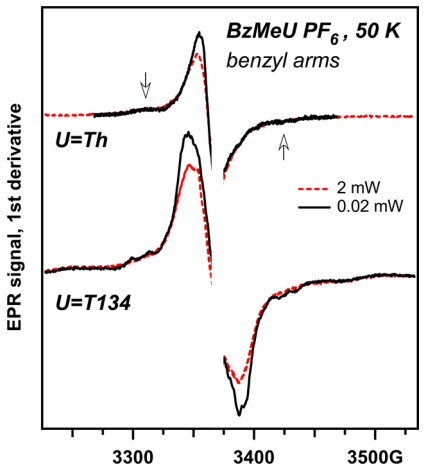

Figure 6. First-derivative EPR spectra observed in irradiated BzMeTh PF_6 and BzMeT134 PF_6 obtained at 50 K, using a microwave power of 0.02 mW (solid line) and 2 mW (dashed line). The arrows indicate the outer resonance lines of the $\mathbf{CH}^{+\bullet}$ radical.

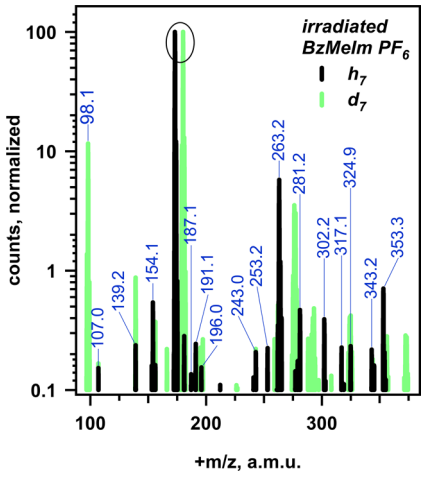

Figure 7. ESI MS_1^+ spectra of room temperature irradiated Bz-x_7–MeIm PF_6, where x = H or D (Table 2). The circle indicates the parent $\mathbf{C}^+$ cation. Note the logarithmic vertical scale.

the MS_1^+ spectra for irradiated BzMeIm PF_6 and Bz-d_7–MeIm PF_6 are overlaid (see also Tables 2 and 8S, Supporting Information). Additional means of cation identification were provided by studying the fragmentation of the mass ions in their collisional excitation. Table 8S (Supporting Information) lists the main neutral fragments and the residual ions obtained in these MS_2^+ experiments.

Due to the use of the isotopomers, BzMeIm PF_6 provided the most complete picture of cation fragmentation. All of the observed positive ions were *monocations*. The main product of radiolysis (with the radiolytic yield G of ~0.84 per 100 eV) is the benzyl adduct to the parent cation ($\mathbf{C}-\mathbf{Bz}^+$). As this species exhibits a mass shift of 13 amu upon d_7-substitution in the benzyl group, the benzyl cation adds to the d_6-phenyl ring of the parent cation. Such a species can also be generated via the *radical* addition of $\mathbf{Bz}^{\bullet}$ to the phenyl ring. These Bz additions can occur repeatedly, as there is also a $\mathbf{C}-\mathbf{Bz}-\mathbf{Bz}^+$ adduct, and it can involve other secondary products (Tables 2 and 8S, Supporting Information). In addition to these reactions, the mass spectra indicate the elimination of a methyl group, as there are several methylated products (Table 2). Other substitutions include −F substitution (apparently, some fluorine atoms generated in radiolytic decomposition of the PF_6^- anion recombine with $\mathbf{C}(-\mathbf{H})^{+\bullet}$ radicals or add to the phenyl ring instead of $H_{1'}$ abstraction). There are also cations "decorated" with 1-methylimidazole and imidazole. The radiolytic yield of these products is ~10% of the yield of $\mathbf{C}-\mathbf{Bz}^+$, and these species could be the products of secondary radiolysis. While the conversion of $\mathbf{C}^+$ to $\mathbf{C}-\mathbf{Bz}^+$ is not negligible, the observed radiolytic yield corresponds to ~1.5% conversion of $BzMeIm^+$ over the entire life cycle of the IL diluent (which corresponds to the projected cumulative radiation dose of 0.5 MGy), and such cations remain as chemically inert as the parent cation. More troublesome is the formation of $\mathbf{C}-\mathbf{MeIm}^+$ conjugates that potentially can interact with metal ions in the solution, but the yield of such radiolytic products is low (0.2% over the life cycle) and such species should be easily protonated in acidic solutions.

Irradiation of BzMeT134 PF_6 also yields $\mathbf{C}-\mathbf{Bz}^+$ cations as the main product of radiolysis (Tables 2 and 8S, Supporting Information), and there are also several other products that are analogous to these for $BzMeIm^+$. In addition, there are several products of phenyl addition suggesting the occurrence of $C_{1'}-C_{2'}$ bond dissociation in the excited state of this cation that does not occur in $BzMeIm^+$. These results suggest that $BzMeT134^+$ is more extensively damaged than $BzMeIm^+$, presenting less interest from a practical standpoint.

For BzMeTh PF_6, the radiolytic yield of $\mathbf{C}-\mathbf{Bz}^+$ is significantly lower than it is for the other two cations (0.35 vs 0.84 per 100 eV) and the main product is, surprisingly, $\mathbf{C}-\mathbf{C}^+$ cation. This result corroborates the suggestion made in section 4.1.2 that the electron adduct of $BzMeTh^+$ undergoes reaction 9 instead of reaction 8. It is likely that the $\mathbf{C}-\mathbf{Bz}^+$ cation in this system is generated mainly through benzyl carbocation addition, which in turn suggests that in $BzMeIm^+$ and $BzMeT134^+$ this carbocation addition accounts for ~40% of cation modification, the rest coming from the benzyl radical reactions.

Turning to 1-alkyl substituted cations (Table 3), there is extensive fragmentation of C−C bonds in the alkyl arms, as there are multiple $\mathbf{C}-\mathbf{Alk}^+$ products of the addition of the corresponding alkyl (Alk) groups to parent cations (~0.8 per 100 eV in total). These reactions involve excited states of the cations that yield carbonium ions, as no matching radicals are observed by EPR spectroscopy. Another commonly occurring substitution is $\mathbf{C}-\mathbf{F}^+$ (0.1–0.26 per 100 eV). The radiolytic product with the highest yield is $\mathbf{C}-\mathbf{C}^+$ and the products of further Alk addition to this cation. The total yield of such products for $BuMeIm^+$ is about 1.0 per 100 eV. Since there is no EPR evidence for C_2-C_2 bond formation in the reduction of $RMeU^+$ radicals for U = Im and T134, it is likely that these $\mathbf{C}-\mathbf{C}^+$ cations are the products of recombination of $\mathbf{C}(-\mathbf{H})^{+\bullet}$ and $\mathbf{C}^{\bullet}$ radicals. Such species have been observed not only for aromatic cations of this kind but also for tetraalkyl ammonium and phosphonium cations.[59] The total loss for these $BuMeIm^+$ cations is ~2.5 species per 100 eV, which is significantly greater

dx.doi.org/10.1021/jp4082432 | J. Phys. Chem. B 2013, 117, 14372–14384

Table 2. Positively Charged Ions Observed in BzMeU PF_6 (U = Im, T134, and Th) Irradiated to Specified Doses at Room Temperature, as Observed Using ESI MS_1^+ and MS_2^+ Spectrometry

U →	Im		T134		Th	
dose (MGy)	2.68	G^b (100 eV)	2.32	G (100 eV)	4.15	G (100 eV)
cation	%[a]		%		%	
BzPr			0.38	*0.05*		
BzBu			0.74	*0.10*		
Bz_2Bu			0.8	*0.10*		
Ph_2CH			0.33	*0.04*		
Ph_2CMe			0.66	*0.09*	0.5	*0.03*
Ph_3C			0.4	*0.05*	1	*0.07*
C−Me	0.73	*0.08*	0.47	*0.06*		
C−F	0.75	*0.08*	0.88	*0.11*	1.6	*0.11*
C−Me−F					0.6	*0.04*
C−U					0.5	*0.03*
C−MeU	0.95	*0.11*	0.7	*0.09*	2.1	*0.15*
C−Bz	7.5	*0.83*	6.3	*0.82*	5	*0.35*
C−Bz−Me	1.3	*0.14*	0.64	*0.08*		
C−Bz−F			0.9	*0.12*		
C−Bz−Bu			1.1	*0.14*		
C−Bz−U					1.6	*0.11*
C−Bz−MeU	0.67	*0.07*	1.9	*0.25*		
C−Bz−Bz	0.87	*0.10*	1.7	*0.22*	2.6	*0.18*
C−C					15.3	*1.06*
total[c]		1.41		2.32		2.13

[a]% yield with regard to C^+ (that is taken for 100%). [b]Estimated radiolytic yield per 100 eV. [c]The total yield of cation decomposition.

Table 3. Positively Charged Ions Observed in RMeU PF_6 (U = Im, T134, and Th; R = Et and Bu) Irradiated to the Specified Dose at Room Temperature, as Observed Using ESI MS_1^+ and MS_2^+ Spectrometry

U →	Im		T134		T134		Th	
R →	Bu		Et		Bu		Bu	
dose (MGy)	2.77	G^b (100 eV)	1.85	G (100 eV)	1.83	G (100 eV)	2.2	G (100 eV)
cation	%[a]		%		%		%	
−Et					0.56	*0.10*		
−Me			0.3	*0.06*	0.51	*0.09*		
C	100		100		100		100	
C−F	2.1	*0.26*	0.5	*0.10*	1.4	*0.26*	0.8	*0.12*
C−Me	1.1	*0.13*	0.95	*0.19*				
C−Et	1.6	*0.20*			0.85	*0.16*		
C−Pr	0.95	*0.12*			1.1	*0.20*		
C−Bu	1.3	*0.16*	0.6	*0.12*			0.6	*0.09*
C−Bu−Me	0.85	*0.10*	0.5	*0.10*	0.6	*0.11*		
C−Bu−Et	0.77	*0.09*						
C−Bu−Bu					0.65	*0.12*		
C−Bu−U					0.95	*0.18*	0.6	*0.09*
C−Me−MeU	0.77	*0.09*			0.6	*0.11*		
C−C	3.4	*0.42*	2.9	*0.59*	3	*0.55*	1.1	*0.83*
C−C−Me	1.2	*0.15*			0.8	*0.15*	5.7	*0.16*
C−C−Et	1.1	*0.13*						
C−C−Pr	1.5	*0.18*						
C−C−Bu	1.2	*0.15*						
C−U−U			1.9	*0.39*				
C−MeU−U			1	*0.20*				
C−C−MeU			2.6	*0.53*				
C−PF4?	0.82	*0.10*						
C−MeU−PF4?	1.7	*0.21*						
C−U−F?			1	*0.20*				
total[c]		2.49		2.48		2.03		1.29

[a]% yield with regard to C^+ (that is taken for 100%). [b]Estimated radiolytic yield per 100 eV. [c]The total yield of cation decomposition.

dx.doi.org/10.1021/jp4082432 | J. Phys. Chem. B 2013, 117, 14372−14384

than 1.4 species per 100 eV for $BzMeIm^+$. The total yield of the products for $BuMeT134^+$ was somewhat lower, ~2.0 species per 100 eV, mainly due to the lower yield of **C−C**−Alk^+ species.

This analysis suggests that for $BuMeIm^+$ the strategy of replacing the alkyl arms with benzyl arms was successful, but these gains are opposed by (i) undesirable side reactions of the benzyl carbocation and (ii) benzyl radical elimination. As a result, the overall damage can even increase; e.g., for $BzMeT134^+$ it is even greater than in $BuMeT134^+$ (2.3 vs 2.03 per 100 eV). The balance between these processes is subtle, and the assessment of radiation stability for a candidate system requires case by case studies.

An unexpected result is relatively low cation damage in the $BuMeTh^+$ cation (the total product yield of ~1.3 per 100 eV; Table 3) for which there is significantly less fragmentation in the long arm than in other 1-alkyl cations. Interestingly, the yield of **C−C**$^+$ is remarkably higher for this cation than for other cations in Table 3, and this may suggest that the reduced yield of the decomposition positively correlates with the electron delocalization suggested in section 4.1.2.

4.2.2. NMR Spectrometry. The MS_1^- spectra of the irradiated samples indicated the formation of $PF_2O_2^-$ and FPO_3^- anions that are the known products of PF_6^- hydrolysis.[71,72] The same two species were also observed in ^{19}F and ^{31}P NMR spectra of the irradiated samples (Table 9S, Supporting Information). Another common product was BF_4^- (observed at −148 ppm) which is generated by etching of borosilicate glass tubes by the released HF.

In addition to these products, there is a large number of resonance lines from fluorine-19 with $\delta(^{19}F)$ between −45 and −65 ppm that have complex coupling patterns (mainly *dd* and *ddt*) indicating coupling to ^{31}P (with $J(^{19}F-^{31}P)$ of 730−780 Hz) and another spin-1/2 nucleus other than proton (with $J(^{19}F-X)$ of 54−58 Hz); see Table 9S (Supporting Information). There are many other resonance lines, most of which are from ^{19}F nuclei that are not coupled to protons (Table 9S, Supporting Information) or other magnetic nuclei. The yield of all these products is very low as compared to the products of hydrolysis (that probably involves reaction intermediates rather than the parent anions). For 1-benzyl substituted cations, there are proton-coupled ^{19}F resonances with $\delta(^{19}F)$ between −117 and −112 ppm with coupling patterns suggestive of F-substitution in the aromatic rings of the parent cation.

As observed in section 4.2.1, for $BzMeIm^+$ and $BzMeT134^+$, the **C−Bz**$^+$ cation is the main radiolytic product. This agrees with the ^1H NMR spectra of irradiated BzMeIm PF_6 (Figures 19S, Supporting Information) that indicate one main group of coupled protons in the 3-methylimidazolium head of the cation that are downfield of the resonance lines of the parent cation. Corresponding resonances from this charged headgroup are also observed in the ^{13}C NMR spectra shown in Figure 20S (Supporting Information), corroborating the previously made assertion (suggested by isotope substitution experiments described in section 4.2.1) that benzyl derivatization occurs in the *benzyl* arm of the parent cation.

Many more reaction products are observed in the ^1H NMR spectra of irradiated BzMeT134 PF_6 (Figure 21S, Supporting Information). The reaction product with the strongest ^1H resonances (group-A) has $^1H_2$ and $^1H_5$ protons that are significantly downfield of the parent cation; the estimated yield of this product is 0.52 per 100 eV. Modified cations can also be observed in the ^{13}C NMR spectra of this irradiated compound (Figure 22S, Supporting Information).

The NMR spectra for irradiated BzMeTh PF_6, like the corresponding MS_1^+ spectra (section 4.2.1), indicate the presence of a single *major* product that is a derivative of the cation with a thiazole group (Figure 23S and 24S and Scheme 2S, Supporting Information). There is also a strong ^{13}C resonance at 42.3 ppm that corresponds to methylene carbon in a benzyl-derivatized phenyl group (Figure 24S, Supporting Information) that is analogous to the 40.8 ppm resonance observed in irradiated BzMeIm PF_6 (Figure 20S, Supporting Information). The MS_1^+ analyses suggest that the main product is the **C−C**$^+$ cation; it appears that the latter species is the product of the attachment of the benzyl to the phenyl ring of the cation, while a MeTh group is attached to this benzyl ring through its C_4 carbon.

Turning to $RMeU^+$ cations with the alkyl groups, the MS_1^+ spectra indicate the presence of multiple products with relatively low yield for each particular product, and this is also suggested by ^1H NMR spectra (e.g., Figures 25S and 26S, Supporting Information, for irradiated BuMeIm PF_6) in which there are at least seven proton-coupled groups. The ^{13}C NMR spectra suggest that these groups arise from differently substituted imidazolium cations (Figure 27S, Supporting Information), with many types of substitution and fragmentation in the side arm. The presence of ^1H resonance lines with $\delta(^1H)$ between 5.5 and 7 ppm suggests fragmentation in the aliphatic arms (with the formation of olefins with the characteristic *J*-couplings) and substituted 1-methylimidazoles. Such products were observed for EtMeT134 PF_6 (Figures 28S and 29S, Supporting Information), but fewer of these products were observed for BuMeT134 PF_6 (Figures 30S and 31S, Supporting Information), for which derivatization of the parent cation prevailed. The same applies to BuMeTh PF_6 (Figure 32S and 33S, Supporting Information), although there are (as for $BuMeIm^+$) many products suggesting multiple fragmentation pathways. Judging from the *J*-couplings (~47 Hz) for protons with $\delta(^1H)$ between 5.5 and 6.5 ppm (Figures 26S, 28S, and 32S, Supporting Information), there is also F-substitution in the aliphatic chains of the cations; however, the majority of the proton resonances exhibit $^1H-^1H$ coupling only.

We conclude that radiolysis of 1-alkyl substituted cations causes multiple fragmentation of C−C and C−N bonds in the aliphatic arms, whereas the fragmentation in 1-benzyl substituted cations is more selective. These reactions spare the aromatic ring of the cation, but some of these reactions result in the loss of positive charge. Since the latter species can escape MS_1^+ detection (while appearing in ^1H and ^{13}C NMR spectra), the total radiolytic yields of cation decomposition given in section 4.2.1 are the *lower* estimates.

5. CONCLUDING REMARKS

To replace conventional molecular diluents in nuclear separations, hydrophobic ionic liquids (ILs) must be stabilized to radiolytic decomposition. This study supports previous results[39,40,42,56,57,59] indicating that organic cations in irradiated ionic compounds undergo extensive fragmentation that results in partial or complete loss of their side aliphatic arms. Our aim is to develop approaches to improving cation stability to such fragmentation reactions. Although the latter cannot be fully suppressed, it is possible to decrease their extent over the expected life cycle of the IL diluent.

dx.doi.org/10.1021/jp4082432 | J. Phys. Chem. B 2013, 117, 14372−14384

We demonstrate that, by stabilization of the carbocation that is released in the dissociation of electronically excited cations derived from 5-membered ring heterocycles, it is possible to reverse this channel of cation fragmentation but only at a cost of increasing the yield of products of carbocation addition to the parent cation. One way of such stabilization is the replacement of 1-alkyl arms with 1-benzyl arms, as the benzyl carbocation is particularly stable. Unfortunately, this substitution also facilitates the elimination of a benzyl radical from the corresponding electron adduct. We observed the latter reaction for 1-benzyl substituted cations of 3-methylimidazolium and 3-methyl-1,3,4-triazolium (Scheme 1), whereas this reaction was not observed for 1-benzyl-5-methylthiazolium and (as shown in part 2) for 1-benzyl-pyridinium.[55] The increased stability for the latter adducts is due to excess electron delocalization over two cations, most likely involving (in the case of 1-R-5-methylthiazolium) C_2-C_2 bound $\sigma^2\sigma^{1*}$ dimer radical cations. While the observed EPR spectra are consistent with this interpretation, further spectroscopic characterization is necessary to confirm it.

Our calculations indicate that thiazolium based cations form such dimer cation species more readily than triazolium and imidazolium based cations due to reduced steric hindrance and trigonality in the corresponding carbon-2 atom. The 1-butyl-5-methylthiazolium and 1-benzyl-3-methylimidazolium cations yield relatively few products in radiolysis of their hexafluorophosphates (1.3−1.4 per 100 eV), whereas for other ionic compounds this yield is 2−2.5 per 100 eV. While 1-benzyl-5-methylthiazolium cations are more stable to benzyl radical elimination, there is a higher yield of dimer cations among the reaction products. Most of these cation modifications (by reactive fragments) increase the hydrophobicity of the product cation, so it is unlikely that the conversion of 1−2% of the parent cations to such products over their life cycle would have a significant effect on the performance of IL diluents in *neutral* extraction (no intended exchange of metal ions in the aqueous phase with organic cations in the IL phase).

While these 1-benzyl derivatives provide only moderate improvement in the overall cation stability, they yield fewer fragments, and therefore exhibit more predictable products than the corresponding 1-alkyl derivatives that undergo multiple C−C bond fission in their aliphatic chains, resulting in numerous cation adducts. The yield of free heterocycle bases and their conjugates is low (Tables 2 and 3). All such species would become protonated even in weakly acidic solutions, once again suggesting limited interference with metal ion extraction. The latter is much more likely to be affected by anion rather than cation fragmentation.

As was noted in the Introduction, the stability of electronically excited cations anticorrelates with the stability of their reduced states. Electron delocalization that is observed in some of the cations improves the latter, but *the same end result can be obtained through competitive electron scavenging that precludes cation reduction.* We demonstrated this strategy for 1-benzyl-3-methylimidazolium (section 4.1.1). When this cation was paired with saccharinate (that preferentially accepts electrons in this system), fragmentation of the cation was prevented, as the electrons were scavenged by the anion in preference to the cation. Introduction of a protic impurity was also sufficient to inhibit this fragmentation.

In a practical setting, the IL diluent remains in continuous contact with the aqueous raffinate. The acidity of the latter alternates during the forward and back extractions,[39] so the IL diluent spends roughly half of its life cycle in contact with acidic (typically, nitric acid) aqueous solutions. As nitric acid and nitrate are efficient electron scavengers, most radiolytically generated electrons are scavenged by hydronium ions and nitric acid/nitrate introduced into the IL.[61] In this part of the cycle, as suggested by our study, the reductive channel to cation fragmentation does not pose a problem. However, acid dopants can protonate bases released in reaction 9, suppressing the reverse reaction. As the latter is a geminate reaction, such interference can occur only when the concentration of the acid is high, which is only possible when the IL diluent is in contact with concentrated acids. Since nitrate and nitric acid also serve as efficient quenchers of electronic excitation,[61] they will also suppress reaction 8, so radiolytic fragmentation of cations in highly acidic ILs is unlikely to be a problem. However, as the proticity decreases during the complementary part of the cycle, the IL diluent also needs to be stabilized to radiation damage under the conditions of low acidity. For this low acidity regime, the intrinsic resistance of the IL to radiation becomes important, and our study suggests several ways in which it can be improved.

■ ASSOCIATED CONTENT

Supporting Information

PDF file containing a list of abbreviations and chemical reactions, synthetic procedures, Schemes 1S and 2S, Tables 1S−9S, and Figures 1S−33S with captions, including radical geometries, experimental and simulated EPR spectra, and NMR spectra. This material is available free of charge via the Internet at http://pubs.acs.org.

■ AUTHOR INFORMATION

Corresponding Author

*E-mail shkrob@anl.gov. Phone: (630) 252-9516.

Notes

The authors declare no competing financial interest.

■ ACKNOWLEDGMENTS

We thank S. Chemerisov, R. Lowers, D. Quigley, S. Lopykinski, and J. Muntean for technical support. The work at Argonne and Oak Ridge was supported by the US-DOE Office of Science, Division of Chemical Sciences, Geosciences and Biosciences under Contract Nos. DE-AC02-06CH11357 and DE-AC05-0096OR22725, respectively. Programmatic support via a DOE SISGR grant "An Integrated Basic Research Program for Advanced Nuclear Energy Separations Systems Based on Ionic Liquids" is gratefully acknowledged.

■ REFERENCES

(1) Welton, T. Room-Temperature Ionic Liquids. Solvents for Synthesis and Catalysis. *Chem. Rev.* **1999**, *99*, 2071−2083.

(2) Smiglak, M.; Metlen, A.; Rogers, R. D. The Second Evolution of Ionic Liquids: From Solvents and Separations to Advanced Materials -Energetic Examples from the Ionic Liquid Cookbook. *Acc. Chem. Res.* **2007**, 1182−1192.

(3) Plechkova, N. V.; Seddon, K. R. Applications of Ionic Liquids in the Chemical Industry. *Chem. Soc. Rev.* **2008**, *37*, 123−150.

(4) Hallett, J. P.; Welton, T. Room-Temperature Ionic Liquids: Solvents for Synthesis and Catalysis. 2. *Chem. Rev.* **2011**, *111*, 3508−3576.

(5) Visser, A. E.; Swatloski, R. P.; Reichert, W. M.; Mayton, R.; Sheff, S.; Wierzbicki, A.; Davis, J. H.; Rogers, R. D. Task-Specific Ionic Liquids for the Extraction of Metal Ions from Aqueous Solutions. *Chem. Commun.* **2001**, 135−136.

(6) Luo, H. M.; Dai, S.; Bonnesen, P. V.; Buchanan, A. C.; Holbrey, J. D.; Bridges, N. J.; Rogers, R. D. Extraction of Cesium Ions from Aqueous Solutions Using Calix[4]Arene-Bis(*tert*-Octylbenzo-Crown-6) in Ionic Liquids. *Anal. Chem.* **2004**, *76*, 3078−3083.
(7) Visser, A. E.; Rogers, R. D. Room-Temperature Ionic Liquids: New Solvents for F-Element Separations and Associated Solution Chemistry. *J. Solid State Chem.* **2003**, *171*, 109−113.
(8) Visser, A. E.; Jensen, M. P.; Laszak, I.; Nash, K. L.; Choppin, G. R.; Rogers, R. D. Uranyl Coordination Environment in Hydrophobic Ionic Liquids: An in Situ Investigation. *Inorg. Chem.* **2003**, *42*, 2197−2199.
(9) Dietz, M. L.; Dzielawa, J. A.; Laszak, I.; Young, B. A.; Jensen, M. P. Influence of Solvent Structural Variations on the Mechanism of Facilitated Ion Transfer into Room-Temperature Ionic Liquids. *Green Chem.* **2003**, *5*, 682−685.
(10) Luo, H. M.; Dai, S.; Bonnesen, P. V. Solvent Extraction of Sr^{2+} and Cs^{+} Based on Room-Temperature Ionic Liquids Containing Monoaza-Substituted Crown Ethers. *Anal. Chem.* **2004**, *76*, 2773−2779.
(11) Gutowski, K. E.; Bridges, N. J.; Cocalia, V. A.; Spear, S. K.; Visser, A. E.; Holbrey, J. D.; Davis, J. H.; Rogers, R. D. Ionic Liquid Technologies for Utilization in Nuclear-Based Separations. In *Ionic Liquids: Fundamentals, Progress, Challenges and Opportunities: Transformations and Processes*; American Chemical Society: Washington, DC, 2005; Vol. *902*, pp 33−48.
(12) Dietz, M. L.; Dzielawa, J. A.; Jensen, M. P.; Beitz, J. V.; Borkowski, M. Mechanisms of Metal Ion Transfer into Ionic Liquids and Their Implications for the Application of Ionic Liquids as Extraction Solvents. In *Ionic Liquids: Fundamentals, Progress, Challenges and Opportunities: Transformations and Processes*; American Chemical Society: Washington, DC, 2005; Vol. *902*, pp 2−18.
(13) Stepinski, D. C.; Jensen, M. P.; Dzielawa, J. A.; Dietz, M. L. Synergistic Effects in the Facilitated Transfer of Metal Ions into Room-Temperature Ionic Liquids. *Green Chem.* **2005**, *7*, 151−158.
(14) Dietz, M. L.; Stepinski, D. C. A Ternary Mechanism for the Facilitated Transfer of Metal Ions into Room-Temperature Ionic Liquids (RTIL): Implications for the "Greenness" of Rtils as Extraction Solvents. *Green Chem.* **2005**, *7*, 747−750.
(15) Gaillard, C.; Moutiers, G.; Mariet, C.; Antoun, T.; Gadenne, B.; Hesemann, P.; Moreau, J. J. E.; Ouadi, A.; Labet, A.; Billard, I. Potentialities of Room Temperature Ionic Liquids for the Nuclear Fuel Cycle: Electrodeposition and Extraction. In *Ionic Liquids Iiib: Fundamentals, Progress, Challenges and Opportunities: Transformations and Processes*; American Chemical Society: Washington, DC, 2005; Vol. *902*, pp 19−32.
(16) Cocalia, V. A.; Jensen, M. P.; Holbrey, J. D.; Spear, S. K.; Stepinski, D. C.; Rogers, R. D. Identical Extraction Behavior and Coordination of Trivalent or Hexavalent F-Element Cations Using Ionic Liquid and Molecular Solvents. *Dalton Trans.* **2005**, 1966−1971.
(17) Nakashima, K.; Kubota, F.; Maruyama, T.; Goto, M. Feasibility of Ionic Liquids as Alternative Separation Media for Industrial Solvent Extraction Processes. *Ind. Eng. Chem. Res.* **2005**, *44*, 4368−4372.
(18) Cocalia, V. A.; Gutowski, K. E.; Rogers, R. D. The Coordination Chemistry of Actinides in Ionic Liquids: A Review of Experiment and Simulation. *Coord. Chem. Rev.* **2006**, *250*, 755−764.
(19) Stepinski, D. C.; Young, B. A.; Jensen, M. P.; Rickert, P. G.; Dzielawa, J. A.; Dilger, A. A.; Rausch, D. J.; Dietz, M. L., Application of Ionic Liquids in Actinide and Fission Product Separations: Progress and Prospects. In *Separations for the Nuclear Fuel Cycle in the 21st Century*; Lumetta, G. J., Nash, K. L., Clark, S. B., Friese, J. I., Eds.; American Chemical Society: Washington, DC, 2006; pp 233−247.
(20) Luo, H. M.; Dai, S.; Bonnesen, P. V.; Haverlock, T. J.; Moyer, B. A.; Buchanan, A. C. A Striking Effect of Ionic-Liquid Anions in the Extraction of Sr^{2+} and Cs^{+} by Dicyclohexano-18-Crown-6. *Solvent Extr. Ion Exch.* **2006**, *24*, 19−31.
(21) Dietz, M. L. Ionic Liquids as Extraction Solvents: Where Do We Stand? *Sep. Sci. Technol.* **2006**, *41*, 2047−2063.
(22) Binnemans, K. Lanthanides and Actinides in Ionic Liquids. *Chem. Rev.* **2007**, *107*, 2592−2614.
(23) Lee, J. S.; Luo, H. M.; Baker, G. A.; Dai, S. Cation Cross-Linked Ionic Liquids as Anion-Exchange Materials. *Chem. Mater.* **2009**, *21*, 4756−4758.
(24) Venkatesan, A. K.; Srinivasan, T. G.; Vasudeva Rao, P. R. A Review on the Electrochemical Applications of Room Temperature Ionic Liquids in Nuclear Fuel Cycle. *J. Nucl. Radiochem. Sci.* **2009**, *10*, R1−R6.
(25) Rout, A.; Venkatesan, K. A.; Srinivasan, T. G.; Vasudeva Rao, P. R. Unusual Extraction of Plutonium(IV) from Uranium(VI) and Americium(III) Using Phosphonate Based Task Specific Ionic Liquid. *Radiochim. Acta* **2010**, *98*, 459−466.
(26) Sun, X. Q.; Bell, J. R.; Luo, H. M.; Dai, S. Extraction Separation of Rare-Earth Ions Via Competitive Ligand Complexations between Aqueous and Ionic-Liquid Phases. *Dalton Trans.* **2011**, *40*, 8019−8023.
(27) Sun, X.; Bell, J. R.; Luo, H.; Dai, S. Extraction Separation of Rare-Earth Ions via Competitive Ligand Complexations between Aqueous and Ionic-Liquid Phases. *Dalton Trans.* **2011**, *40*, 8019−8023.
(28) Rout, A.; Venkatesan, K. A.; Srinivasan, T. G.; R., V. R. P. Extraction and Third Phase Formation Behavior of Eu(III) in CMPO−TBP Extractants Present in Room Temperature Ionic Liquid. *Sep. Purif. Technol.* **2011**, *76*, 238−243.
(29) Yu, B.; Bell, J. R.; Luo, H.; Dai, S. Ionic Liquid and Silica Sol-Gel Composite Materials Doped with Todga for the Extraction of La^{3+} and Ba^{2+}. *Sep. Sci. Technol.* **2012**, *47*, 244−249.
(30) Luo, H. M.; Boll, R. A.; Bell, J. R.; Dai, S. Facile Solvent Extraction Separation of Th-227 and Ac-225 Based on Room-Temperature Ionic Liquids. *Radiochim. Acta* **2012**, *100*, 771−778.
(31) Sun, X. Q.; Luo, H. M.; Dai, S. Ionic Liquids-Based Extraction: A Promising Strategy for the Advanced Nuclear Fuel Cycle. *Chem. Rev.* **2012**, *112*, 2100−2128.
(32) Panja, S.; Mohapatra, P. K.; Tripathi, S. C.; Gandhi, P. M.; Janardan, P. A Highly Efficient Solvent System Containing Todga in Room Temperature Ionic Liquids for Actinide Extraction. *Sep. Purif. Technol.* **2012**, *96*, 289−295.
(33) Billard, I.; Ouadi, A.; Gaillard, C. Liquid-Liquid Extraction of Actinides, Lanthanides, and Fission Products by Use of Ionic Liquids: From Discovery to Understanding. *Anal. Bioanal. Chem.* **2011**, *400*, 1555−1566.
(34) Kolarik, Z. Ionic Liquids: How Far Do They Extend the Potential of Solvent Extraction of F-Elements? *Solvent Extr. Ion Exch.* **2013**, *31*, 24−60.
(35) Mohapatra, P. K.; Sengupta, A.; Iqbal, M.; Huskens, J.; Verboom, W. Diglycolamide-Functionalized Calix[4]Arenes Showing Unusual Complexation of Actinide Ions in Room Temperature Ionic Liquids: Role of Ligand Structure, Radiolytic Stability, Emission Spectroscopy, and Thermodynamic Studies. *Inorg. Chem.* **2013**, *52*, 2533−2541.
(36) Billard, I.; Ouadi, A.; Gaillard, C. Is a Universal Model to Describe Liquid−Liquid Extraction of Cations by Use of Ionic Liquids in Reach? *Dalton Trans.* **2013**, *42*, 6203−6212.
(37) Berthon, L.; Chabronnel, M.-C. Radiolysis of Solvents Used in Nuclear Fuel Reprocessing. In *Ion Exchange and Solvent Extraction, A Series of Advances*; Moyer, B. A., Ed.; CRC Press: Boca Raton, FL, 2010; Vol. *19*, pp 429−513.
(38) Allen, D.; Baston, G.; Bradley, A. E.; Gorman, T.; Haile, A.; Hamblett, I.; Hatter, J. E.; Healey, M. J. F.; Hodgson, B.; Lewin, R.; Lovell, K. V.; Newton, B.; Pitner, W. R.; Rooney, D. W.; Sanders, D.; Seddon, K. R.; Sims, H. E.; Thied, R. C. An Investigation of the Radiochemical Stability of Ionic Liquids. *Green Chem.* **2002**, *4*, 152−158.
(39) Berthon, L.; Nikitenko, S. I.; Bisel, I.; Berthon, C.; Faucon, M.; Saucerotte, B.; Zorz, N.; Moisy, P. Influence of Gamma Irradiation on Hydrophobic Room-Temperature Ionic Liquids [BuMeIm] PF_6 and [BuMeIm]$(CF_3SO_2)_2N$. *Dalton Trans.* **2006**, 2526−2534.
(40) Bosse, E.; Berthon, L.; Zorz, N.; Monget, J.; Berthon, C.; Bisel, I.; Legand, S.; Moisy, P. Stability of $[MeBu_3N][Tf_2N]$ under Gamma Irradiation. *Dalton Trans.* **2008**, 924−931.

(41) Yuan, L. Y.; Peng, J.; Xu, L.; Zhai, M. L.; Li, J. Q.; Wei, G. S. Influence of Gamma-Radiation on the Ionic Liquid [C(4)mim][PF_6] During Extraction of Strontium Ions. *Dalton Trans.* **2008**, 6358−6360.
(42) Le Rouzo, G.; Lamouroux, C.; Dauvois, V.; Dannoux, A.; Legand, S.; Durand, D.; Moisy, P.; G., M. Anion Effect on Radiochemical Stability of Room-Temperature Ionic Liquids under Gamma Irradiation. *Dalton Trans.* **2009**, 6175−6184.
(43) Tarabek, P.; Shengyan, L.; Haygarth, K.; Bartels, D. M. Hydrogen Gas Yields in Irradiated Room-Temperature Ionic Liquids. *Radiat. Phys. Chem.* **2009**, *78*, 168−172.
(44) Yuan, L. Y.; Xu, C.; Peng, J.; Xu, L.; Zhai, M. L.; Li, J. Q.; Wei, G. S.; Shen, X. H. Identification of the Radiolytic Product of Hydrophobic Ionic Liquid [C4mim][NTf_2] During Removal of Sr^{2+} from Aqueous Solution. *Dalton Trans.* **2009**, 7873−7875.
(45) Yuan, L. Y.; Peng, J.; Xu, L.; Zhai, M. L.; Li, J. Q.; Wei, G. S. Radiation Effects on Hydrophobic Ionic Liquid [C_4mim][NTf_2] During Extraction of Strontium Ions. *J. Phys. Chem. B* **2009**, *113*, 8948−8952.
(46) Yuan, L.; Peng, J.; Xu, L.; Zhai, M.; Li, J.; Wie, G. Radiation-Induced Darkening of Ionic Liquid [C_4mim][NTf_2] and Its Decoloration. *Radiat. Phys. Chem.* **2009**, *78*, 1133−1136.
(47) Wishart, J. F. Ionic Liquids and Ionizing Radiation: Reactivity of Highly Energetic Species. *J. Phys. Chem. Lett.* **2010**, *1*, 3225−3231.
(48) Ha, S. H.; Menchavez, R. N.; Koo, Y.-M. Reprocessing of Spent Nuclear Waste Using Ionic Liquids. *Korean J. Chem. Eng.* **2010**, *27*, 1360−1365.
(49) Jagadeeswara Rao, C.; Venkatesan, K. A.; Tata, B. V. R.; Nagarajan, K.; Srinivasan, T. G.; Vasudeva Rao, P. R. Radiation Stability of Some Room Temperature Ionic Liquids. *Radiat. Phys. Chem.* **2011**, *80*, 643−649.
(50) Wishart, J. F. Ionic Liquid Radiation Chemistry. In *Ionic Liquids: Coiled for Action*; Seddon, K. R., Rogers, R. D., Eds.; Wiley, Ltd.: Chichester, U.K., 2013; in press.
(51) Dhiman, S. B.; Goff, G. S.; Runde, W.; LaVerne, J. A. Hydrogen Production in Aromatic and Aliphatic Ionic Liquids. *J. Phys. Chem. B* **2013**, *117*, 6782−6788.
(52) Shkrob, I. A.; Chemerisov, S. D.; Wishart, J. F. The Initial Stages of Radiation Damage in Ionic Liquids and Ionic Liquid-Based Extraction Systems. *J. Phys. Chem. B* **2007**, *111*, 11786−11793.
(53) Shkrob, I. A.; Wishart, J. F. Charge Trapping in Imidazolium Ionic Liquids. *J. Phys. Chem. B* **2009**, *113*, 5582−5592.
(54) Shkrob, I. A. Deprotonation and Oligomerization in Photo-, Radiolytically, and Electrochemically Induced Redox Reactions in Hydrophobic Alkylalkylimidazolium Ionic Liquids. *J. Phys. Chem. B* **2010**, *114*, 368−375.
(55) Shkrob, I. A.; Marin, T. W.; Wishart, J. F. Radiation Stability of Cations in Ionic Liquids. 2. Improved Radiation Resistance through Charge Delocalization in 1-Benzylpyridinium. *J. Phys. Chem. B* **2013**, DOI: 10.1021/jp408242b.
(56) Shkrob, I. A.; Marin, T. W.; Chemerisov, S. D.; Hatcher, J. L.; Wishart, J. F. Radiation Induced Redox Reactions and Fragmentation of Constituent Ions in Ionic Liquids. 2. Imidazolium Cations. *J. Phys. Chem. B* **2011**, *115*, 3889−3902.
(57) Shkrob, I. A.; Marin, T. W.; Chemerisov, S. D.; Wishart, J. F. Radiation-Induced Redox Reactions and Fragmentation of Constituent Ions in Ionic Liquids. I. Anions. *J. Phys. Chem. B* **2011**, *115*, 3872−3888.
(58) Shkrob, I. A.; Marin, T. W.; Chemerisov, S. D.; Hatcher, J. L.; Wishart, J. F. Toward Radiation-Resistant Ionic Liquids. Radiation Stability of Sulfonyl Imide Anions. *J. Phys. Chem. B* **2012**, *116*, 9043−9055.
(59) Shkrob, I. A.; Marin, T. W.; Wishart, J. F. Ionic Liquids Based on Polynitrile Anions: Hydrophobicity, Low Proton Affinity, and High Radiolytic Resistance Combined. *J. Phys. Chem. A* **2013**, *117*, 7084−7094.
(60) Shkrob, I. A.; Wishart, J. F. Free Radical Chemistry in Room-Temperature Ionic Liquids. In *Encyclopedia of Radicals in Chemistry, Biology and Materials*; Chatgilialoglu, C., Studer, A., Eds.; John Wiley & Sons, Ltd.: Chichester, U.K., 2012; pp 433−448.
(61) Shkrob, I. A.; Marin, T. W.; Chemerisov, S. D.; Wishart, J. F. Radiation and Radical Chemistry of NO_3^-, HNO_3, and Dialkylphosphoric Acids in Room-Temperature Ionic Liquids. *J. Phys. Chem. B* **2011**, *115*, 10927−10942.
(62) Kabi, A.; Clay, P. G. Gamma Radiolysis of Aqueous Solutions of Aryl Alkyl Amines. *Radiat. Res.* **1968**, *34*, 680−688.
(63) Bobrowski, K. Pulse Radiolysis of Aqueous Solutions of Benzyltrialkylammonium Cations: Reactions with the Primary Transients from Water Radiolysis. *J. Phys. Chem.* **1981**, *85*, 381−388.
(64) Mittal, L. J.; Mittal, J. P. Site of Attack in the Interaction of Hydrated Electrons and Hydroxy Radicals in the Pulse Radiolysis of Arylalkylamines in Aqueous Solutions. *Radiat. Phys. Chem.* **1986**, *28*, 363−371.
(65) Hillesheim, P. C.; Mahurin, S. M.; Fulvio, P. F.; Yeary, J. S.; Oyola, Y.; Jiang, D.; Dai, S. Synthesis and Characterization of Thiazolium-Based Room Temperature Ionic Liquids for Gas Separations. *Ind. Eng. Chem. Res.* **2012**, *51*, 11530−11537.
(66) Hillesheim, P. C.; Singh, J. A.; Mahurin, S. M.; Fulvio, P. F.; Oyola, Y.; Zhu, X.; Jiang, D.; Dai, S. Effect of Alkyl and Aryl Substitutions on 1,2,4-Triazolium Based Ionic Liquids for Carbon Dioxide Separation and Capture. *RSC Adv.* **2013**, *3*, 3981−3989.
(67) Becke, A. D. Density-Functional Exchange-Energy Approximation with Correct Asymptotic Behavior. *Phys. Rev. A* **1988**, *38*, 3098−3100.
(68) Lee, C.; Yang, W.; Parr, R. G. Development of the Colle-Salvetti Correlation-Energy Formula into a Functional of the Electron Density. *Phys. Rev. B* **1988**, *37*, 785−789.
(69) Frisch, M. J.; Trucks, G. W.; Schlegel, H. B.; Scuseria, G. E.; Robb, M. A.; Cheeseman, V. G.; Montgomery, J. A., Jr.; Vreven, K. N.; Kudin, J. C.; Burant, J. C. *Gaussian 03*, rev. C.02; Gaussian, Inc.: Wallingford, CT, 2004.
(70) Shkrob, I. A.; Marin, T. W.; Crowell, R. A.; Wishart, J. F. Photo- and Radiation- Chemistry of Halide Anions in Ionic Liquids. *J. Phys. Chem. A* **2013**, *117*, 5742−5756.
(71) Swatloski, R. P.; D., H. J.; Rogers, R. D. Ionic Liquids Are Not Always Green: Hydrolysis of 1-Butyl-3-Methylimidazolium Hexafluorophosphate. *Green Chem.* **2003**, *3*, 361−363.
(72) Freire, M. G.; Neves, C. M. S. S.; Marrucho, I. M.; Coutinho, J. A. P.; Fernandes, A. M. Hydrolysis of Tetrafluoroborate and Hexafluorophosphate Counter Ions in Imidazolium-Based Ionic Liquids. *J. Phys. Chem. A* **2010**, *114*, 3744−3749.